*minerals*

*Article*

# Basin Evolution and Massive Sulfide Deposition at Rammelsberg (Germany): Updating the Subsidence Analysis

**Carmen Moreno *, Felipe González and Reinaldo Sáez**

Departamento de Ciencias de La Tierra, University of Huelva, 21071 Huelva, Spain; fbarrio@uhu.es (F.G.); saez@uhu.es (R.S.)

* Correspondence: carmor@uhu.es; Tel.: +34-959-219-813

Received: 21 November 2018; Accepted: 4 January 2019; Published: 14 January 2019

**Abstract:** The Rammelsberg sulfide deposit is classically considered as a SEDEX-type deposit. The origin of SEDEX-type massive sulfides links with the evolution of their hosting basins. They frequently constitute the source for the metal-enriched basinal brines transported afterwards as mineralizing hydrothermal fluids. This study revisits previous data concerning the analysis of the basin that hosts the Rammelsberg deposit, the Goslar basin, updating its subsidence analysis and providing new tectonic and total subsidence curves from two different paleogeographic locations: the depocenter and the basin margin. The basin evolution is defined by five stages depicting different subsidence intensity and mechanisms for each of these locations. The stratigraphic position of Rammelsberg coincides with a drastic change in the basin evolution. A rapid tectonic subsidence event is proposed as a trigger mechanism for hydrothermal activity. The paleogeographic location and the relation between supply of mineralizing fluids and sedimentation rate were critical for the concentration or dissemination of sulfides.

**Keywords:** basin analysis; subsidence; SEDEX; Rammelsberg; Rhenohercynian

## 1. Introduction

The origin of mineral deposits hosted by sedimentary rocks links with the evolution of their hosting basins. Tectonic history and subsidence together with depositional environment, paleogeography, and sediment infill exert a strong influence over the size, location, and nature of ore deposits. For this reason, the sedimentary basin analysis is gaining importance in mineral exploration [1]. In syngenetic ore deposits (i.e., SEDEX or VMS), hosting rock deposition and mineralizing processes are coeval, so that the ore deposit must be interpreted as another lithostratigraphic unit of the basin infill. In consequence, the basin analysis techniques that correlate sedimentation and time can be applied to this type of mineralization, as Maynard and Klein [2] and Large [3] successfully did. However, in epigenetic deposits (e.g., MVT or Kupferschiefer), mineralization postdates sedimentation of the hosting rocks because the ore is generated by postsedimentary pore infill and replacement processes. In these cases, techniques derived from sequence stratigraphy [4] are considered more suitable for exploring the connection between mineralization and sedimentary basin [1].

The space available for potential sediment accumulation, i.e., the accommodation, according to Jervey [5], is probably the most relevant parameter in sedimentary basin analysis because it implicitly incorporates the basin concept itself. Subsidence is one of the major factors controlling the accommodation of marine sedimentary basins and the main one in non-marine basins. In this regard, the analysis of subsidence curves is commonly used to investigate the variation through time of the basin accommodation space, the accommodation rate. Given that factors controlling this rate are mostly related to synsedimentary tectonic processes, the subsidence curves can also explain the geodynamic evolution of sedimentary basins [6–8] including, paradoxically, those tectonically stable [9].

Subsidence analysis is a methodology widely employed in the study of basins of very different ages and origins, particularly in relation to hydrocarbon exploration [10–14]. It is also increasingly used in land planning, specifically, in the identification and quantification of subtle accommodation changes anthropically related [15–18]. In these cases, the subsidence curves are elaborated following the same criteria and procedures that apply to old sedimentary basins, although employing historical times and providing displacement velocities expressed in mm/month or cm/year. Nevertheless, the use of subsidence analysis in the study of sedimentary basins hosting ore deposits is unusual, despite the fact that sedimentation rate, and even subsidence nature, are considered key parameters in the preservation of such ore deposits [19]. This applies even to ore deposits strongly influenced by sedimentary processes, such as BIF [20,21].

In this regard, the pioneer study by Large [3,22] related the genesis of the massive sulfide deposits of Rammelsberg and Meggen with the evolution of the German Rhenohercynian basin. By mean of subsidence analysis, this author positioned Rammelsberg and Meggen deposits in two sharp inflexions of the subsidence curve. These inflexions were interpreted as sporadic tectonic pulses disturbing a slow and extended thermal subsidence phase (post-rift phase). The evolution of the Rhenohercynian basin was thus forced to conform to the theoretical model of isostatic adjustment by McKenzie [23], and the tectonic pulses were therefore conceived as anomalies that disrupted the post-rift phase.

Maynard and Klein [2] successfully applied this subsidence analysis methodology to three sedimentary basins intentionally different in size and origin, all including sizable mineral deposits. These were the Witwatersrand foreland basin (hosting the Witwatersrand Au ore), the Keweenaw rift basin (hosting the White Pine Cu ore), and the strike-slip Huayacocotla basin (hosting the Molango Mn deposit). Similar to what occurred in the Rhenohercynian basin, the three mineral deposits occurred as inflexions of the respective subsidence curves. The authors suggested that none of the curves could be easily explained with a theoretical model, given that each basin followed its own distinctive and commonly complex subsidence history.

Although these studies were innovative and provided highly relevant data, there is still room for improvement, particularly in the application of the method, data management, and interpretations. The basins were conceived in these papers as homogeneous lithospheric portions, and even those with a complex evolution studied by Maynard and Klein [2] were assumed uniform in their complexity. In this regard, the lateral thickness and facies changes, as well as the variability and intensity of the subsiding mechanisms in different parts of the basin must be definitely considered, [24–27].

The subsidence curves by Maynard and Klein [2] and Large [3] were based on compiled regional stratigraphic columns. In the last case, the column integrated the massive sulfide deposits of Rammelsberg and Meggen, notwithstanding that both ores are located in separate areas, and included in different local stratigraphic series. On the other hand, none of the subsidence curves of these authors make the distinction between tectonic and total subsidence/accommodation, despite the fact that this is a simple way to illustrate the combined effect of the different subsidence mechanisms involved in a given time [28].

In this study, we revisit the German Rhenohercynian Zone, elaborating the subsidence curves in the depocenter and margin of the so-called Goslar Trough, the basin that hosts the massive sulfide deposits of Rammelsberg. The subsidence mechanisms and accommodation rates affecting each of these areas in a given time are compared. This allows us to investigate, not only the interrelation between sulfide deposits, hydrothermal activity (heat flow), and geodynamic evolution of the mineralized area, but also the potentiality of other parts of the basin in the generation of mineralizations. Rammelsberg was selected as a case of study because it is a synsedimentary ore deposit, has a very good stratigraphic and chronostratigraphic control, and is fairly well known to be of interest to the scientific community. Other synsedimentary ore deposits could also be analyzed using the same methodology here applied.

## 2. Geological Setting

The Rammelsberg massive sulfide deposit is located in the Upper Harz, the northernmost domain of the Harz Mountains at the German Rhenohercynian Zone, European Variscan Orogen (Figure 1). It represents a non-metamorphosed Devonian–Carboniferous Shale Belt [29]. The Harz Mountains consist of a faulted block, mostly composed of Devonian and Carboniferous rocks, that is bounded by Permian, Mesozoic, and Cenozoic deposits uplifted during the Cretaceous and Paleogene [30]. Its stratigraphic record includes pre- and synorogenic sedimentary rocks, and in minor extent, volcanics and mineral deposits of sulfides and barite. All these rocks were deformed during the main compressive Variscan phase (Mississippian), conforming a fold-and-thrust belt [31,32]. The metamorphic grade was very low. Finally, Permian, post-Variscan intrusions completed the regional geological framework.

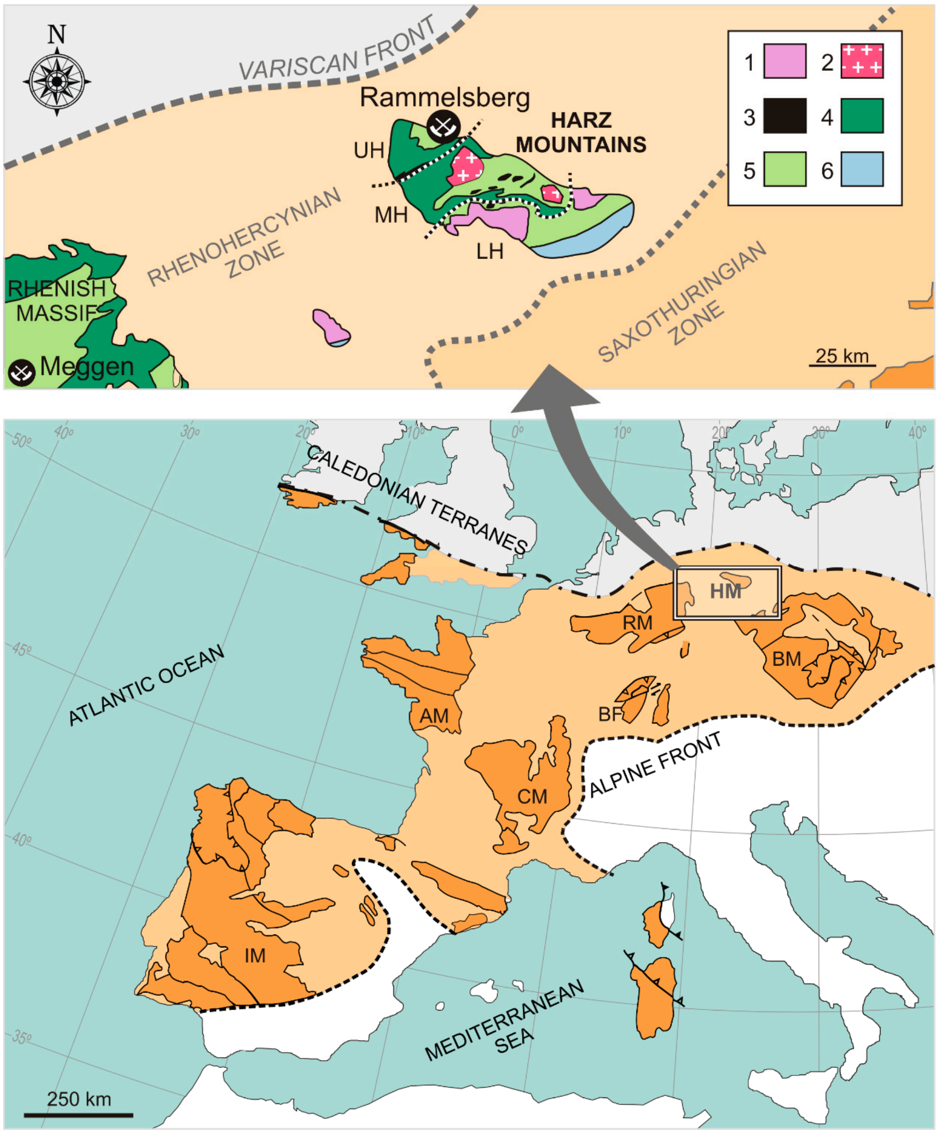


**Figure 1.** Sketch of the European Varican Belt with indication of the major massifs and geological map of the Harz Mountains showing the location of the Rammelsberg and Meggen massive sulfides. Abbreviations: AM, Armorican Massif; BF, Black Forest; BM, Bohemian Massif; CM, Central Massif; HM, Harz Mountains; IM, Iberian Massif; RM, Rhenish Massif; LH, Lower Harz; MH, Middle Harz; UH, Upper Harz. Legend: 1, Permian deposits; 2, Permian granitic rocks; 3, Devonian–Mississippian basic rocks; 4, Carboniferous shales and graywackes; 5, Middle Devonian sand-banded and calcareous shales; 6, pre-Devonian sedimentary rocks.

The location of the Rammelsberg deposit is related to the Devonian paleogeography, which in turn was controlled by the onset of the Variscan Orogeny Cycle in the region [33]. In detail, the phase involved was the initial Variscan rifting stage [34,35], which regionally correlates with the Lower Devonian aperture of the Rhenohercynian Ocean [36]. The intense extensional phase associated with this rifting produced substantial crustal thinning and rupture of the hitherto uniform platform. This involved the activation of extensional faults, deeply rooted in the crust, that generated sub-basins and channeled mineralizing fluids up to the ocean floor [36,37]. The resulting tectonic and paleogeographic scenario during the Middle and Late Devonian entailed different basins bordered by ridges with very different subsidence rates [38]. In the case of Rammelsberg, the massive sulfides are located in the ridge of the Goslar basin (Figure 2), the fault system involved was the Balve–Obersheld fault zone [33], and the fractured and stretched platform is represented by the Emsian Kahleberg Formation. The stratigraphic records of the ridge and depocenter of the Goslar basin represent, respectively, condensed and expanded sequences when compared (Figure 3).

The Goslar basin infill began with the deposition of the Calceola Shales, a lower Eifelian fossiliferous limestone-dominated unit with regional stratigraphic significance. Immediately above is the Eifelian to middle Givetian Wissenbach Shales, the unit that hosts the sulfide deposits. It consists of a shale-dominated sequence interbedded by cm- to dm-thick tuffs of different nature and sandstones, and cm-thick limestone layers. At the base, this unit shows evidence of tectonic instability, including intraformational breccias, synsedimentary faults, and slides [39]. The massive sulfides, located around the middle part of the unit, have been dated as middle Eifelian (*partitus* to *costatus* conodont Zone) by Buchholz and Luppold [40]. Above the Wissenbach Shales are the Banded Shales, a limestone–shale unit Middle Givetian–Frasnian in age including nodular limestones and the Kellwasser horizon. The top of the sequence contains early Mississippian Culm-related flysch deposits, composed mostly of graywackes and shales. Below the sediment pile, the Lower Devonian sandstone-dominated Kahleberg Formation represents the basement substrate. This records the deposition on the continental margin previous to the Goslar basin occurrence [38]. Additional details about all these deposits can be found in Hannak [41], Sperling [42], and Large and Walcher [39].

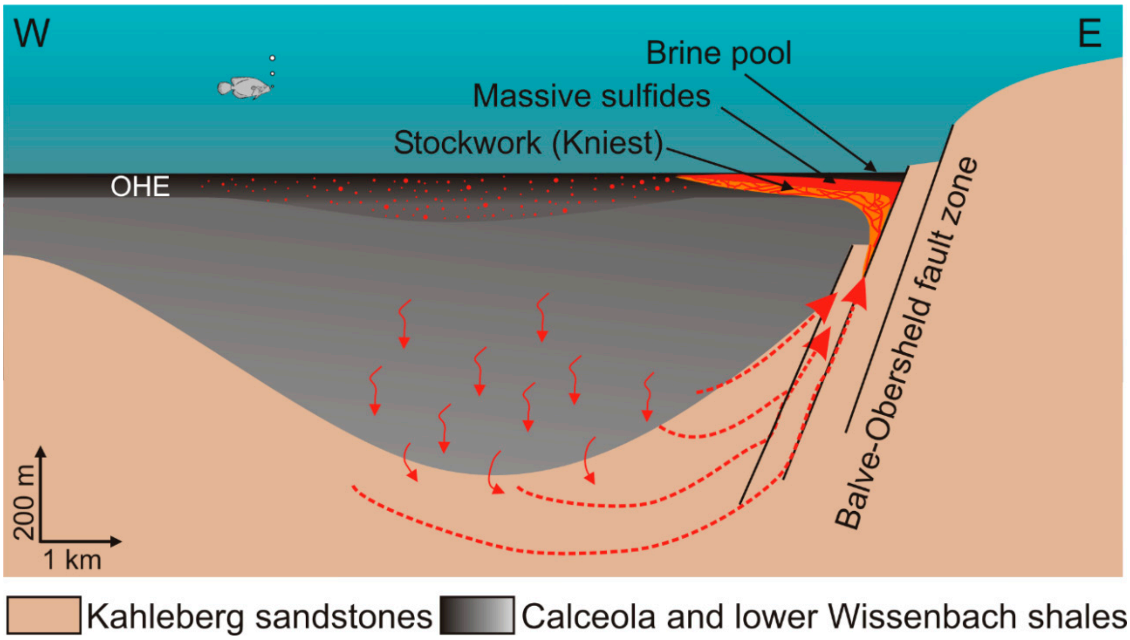


**Figure 2.** Proposed paleogeographic model for the Goslar Basin at the massive sulfide deposition time (middle Eifelian). Red arrows indicate pathways of basinal fluids. OHE; Ore horizon equivalent. Modified from Hannak [41] and Sáez et al. [38].

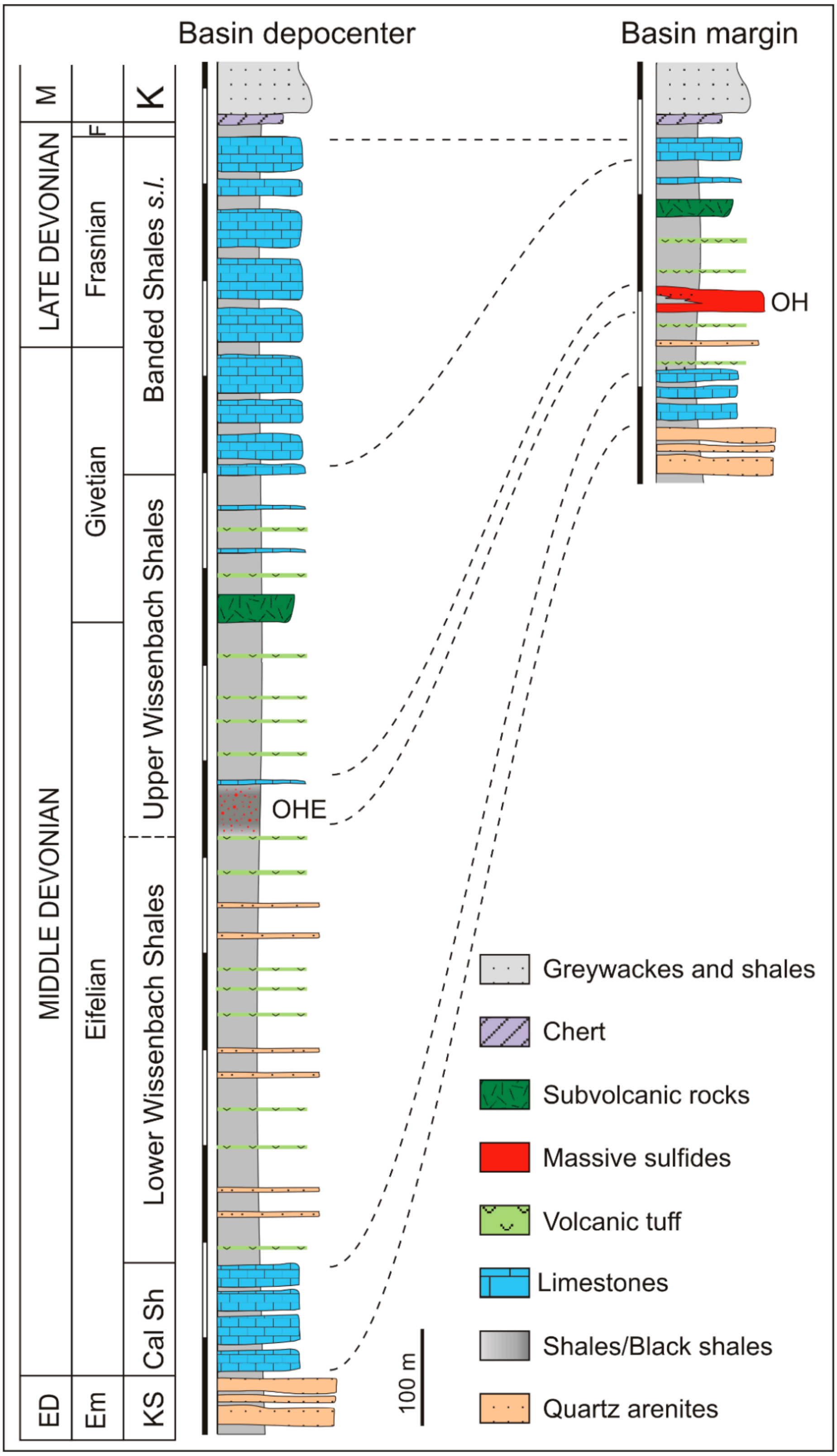


**Figure 3.** Correlation between the stratigraphic logs at the basin depocenter and basin margin. Abbreviations: KS, Kahleberg sandstones; Cal Sh, Calceola Shales; OH, Ore horizon; OHE, Ore horizon equivalent; K, Culm-related deposits; Em, Emsian; F, Famennian; ED, Early Devonian; M, Mississippian. Data based on Buchholz and Luppold [40], Hannak [41], Sperling [42], Large and Walcher [39], and Abt [43].

## 3. Rammelsberg Deposit

The Rammelsberg deposit encompasses several Pb–Zn–Ba-rich massive sulfide lenses, and an overlaying barite body (Grey Ore) with low metal content (4% Cu + Pb + Zn, 80% barite) [44]. A silicified and carbonated zone (called Kniest and interpreted as the feeder zone) underlies the massive sulfides. This is associated with a fault zone thought as the main channel for hydrothermal fluids circulation. In contrast to VMS-type deposits, the feeder zone in Rammelsberg lacks primary metallic mineralization, although it contains some metallic grade related to late veins. According to Muller [29] it contains 2.5 Mt @ 1.3% Cu, 3% Zn, 1.4% Pb, 28 g/t Ag. The alteration related to the Kniest is represented by the association quartz–iron rich chlorite–sericite, and an external carbonated fringe including Mn-rich ankerite and siderite. Mining operations in Rammelsberg have occurred almost continuously from the 10th century until 1988. Original reserves have been estimated at 27–30 Mt @ 14% Zn, 6% Pb, 2% Cu, 140 g/t Ag, 1 g/t Au, and 20% barite [39]. The mineralogy essentially consists of sphalerite, galena, pyrite, barite, and small amounts of chalcopyrite, tetrahedrite–tennantite, freibergite, bornite, and arsenopyrite. As occur in most of the SEDEX deposits, the ore is fine grained and shows frequent massive to banded structure. Replacement and overgrowing textures are also common.

Traditionally, Rammelsberg has been considered representative of vent-proximal SEDEX-type deposits [45]. However, its general high grade, particularly notorious for Cu and Au, puts some doubts in such assignation. Its classification within the Shale Hosted Deposits [46] could explain such geochemical peculiarity [19].

The origin of Rammelsberg, as many other SEDEX-type deposits, is related to the exhalation of hydrothermal fluids in the sea bottom derived from metal-enriched basin brines. Metal enrichment was caused by water/rock interaction processes in a geothermal anomalous environment, presumably related with the magmatic activity that represented, at basin scale, the volcanic rocks interbedded in the sedimentary pile [3,33,41,42]. Sulfur isotopes [47,48] show a wide range of values for pyrite ($\delta^{34}S$ between −20 and +20‰ with the average around +5‰). Average values for galena and sphalerite point to a heavier S, with $\delta^{34}S$ between +5 and +20‰ and the average around +15‰. Negative values are associated with primary textures (framboidal and coloforms) preserved mostly in pyrite. They represent the S component derived from bacterial sulfate reduction (BSR). The heaviest S values are related to the sulfide sulfur supplied by hydrothermal fluids [48]. The origin of this S has been associated with the inorganic reduction of sulfate from intrapore fluids at relatively high temperatures [29]. Nielsen [49] proposed two sources for the reduced S, one derived from BSR processes and the other hydrothermal, this with more homogeneous values. The $\delta^{34}S$ in barite, around +20‰, represents the signature of the Devonian marine sulfate [47,49].

Isotopic data of the Re–Os and Pb–Pb systems [29,50,51] suggest deep circulation of the hydrothermal fluids and interaction with a strongly radiogenic source that has been associated with the Lower Devonian sandstones and the paragneisses of the pre-Variscan substrate [29]. Reduced and metal-enriched fluids could remain in permeable layersand come up to the sea bottom in pulses triggered by the seismotectonic activity associated with the basin evolution.

## 4. Methodology

The performed subsidence analysis followed the classical one-dimensional backstripping technique by Stekler and Watts [52] and Van Hinte [53] by which the sediment and water loadings, interpreted as simple eustatic effects, are removed from the tectonic subsidence. The procedure and parameters applied followed those described by Sclater and Christie [54], Bond and Kominz [55], Angevine et al. [28], Allen and Allen [56], and Hölzel et al. [57], among others. Subsidence analysis was performed using an Excel worksheet according to the procedure indicated by Van Hinte [53] and Allen and Allen [56]. Density, initial porosity, and lithologic constants here applied were directly calculated taking into account the relative proportion of each lithology in each stratigraphic unit. Required stratigraphic data were extracted from the descriptions by Hannak [41], Sperling [42], Large and Walcher [39], and Sáez et al. [38], and complemented by the authors directly in the field. Biostratigraphic data of Buchholz and Luppold [40] provided very precise age data on the units preceding the mineralization. Geochronologic ages were obtained from Weddige [58,59] and Kaufmann [60] for the Devonian, and Menning et al. [61] for the Carboniferous.

The subsidence curves were elaborated omitting depth of deposition and eustatic sea level. The assumed error was nevertheless negligible, because the water column remained roughly constant through time, as suggested by sedimentary facies and fossil associations. By contrast, the denuded Culm series was taken into account by estimating an average thickness of 2000 m, according to available data on the European Variscan flysch [62].

## 5. Subsidence Analysis

Total subsidence curves for the depocenter and margin of the Goslar basin are shown in Figure 4. Both include tectonic subsidence and total accommodation. Each curve is composed of five pairs of segments defined by the five time intervals considered in this study. They correspond to stratigraphic units or to changes in the sedimentary facies of the stratigraphic record. These are: (1) Calceola Shales; (2) Lower Wissenbach Shales; (3) Upper Wissenbach Shales, with the sulfide deposits at the base; (4) Banded Shales; and (5) Culm-related flysh sequences. Each pair of segments (tectonic subsidence plus total accommodation) defines a subsidence stage (Figure 4, Table 1). Parameters such as parallelism or divergence, slope and relative length of the segments provide information about the geodynamic evolution of the basin and the mechanisms responsible for the total accommodation in each stage. The average accommodation rates calculated for the basin margin and depocenter in each stage are also included in Table 1.

**Table 1.** Stages conforming the subsidence curves from Rammelsberg ridge and Goslar depocenter with indication of the accommodation rates and subsidence mechanisms proposed for each case. The red line specifies the location of the massive sulfides. Abbreviations: AC, Accommodation rates; Tec, Tectonic subsidence.

| Stages | Time Span (ma) | Stratigraphic Units | Rammelsberg Ridge | | | Goslar Depocenter | | |
|---|---|---|---|---|---|---|---|---|
| | | | AC (cm/ka) | Accommodation Mechanisms | Tec. (%) | AC (cm/ka) | Accommodation Mechanisms | Tec. (%) |
| 5 | 34.7 | Culm related units | 5.9 | Sediment load and tectonic | **43** | 5.9 | Sediment load and tectonic | **19** |
| 4 | 26.5 | Banded Shales *s.l.* | 0.1 | Sediment load + tectonic (minimal) | **45** | 2.5 | Sediment load and tectonic | **37** |
| 3 | 3.9 | Upper Wissenbach Shales | 7.7 | Tectonic and thermal flux | **63** | 17.4 | Sediment load and tectonic | **43** |
| 2 | 0.3 | Lower Wissenbach Shales | 34.1 | Tectonic and thermal flux | **62** | 271.5 | Tectonic and Sediment load | **58** |
| 1 | 0.6 | Calceola Shales | 24.5 | Mainly tectonic | **70** | 53.9 | Mainly tectonic | **70** |

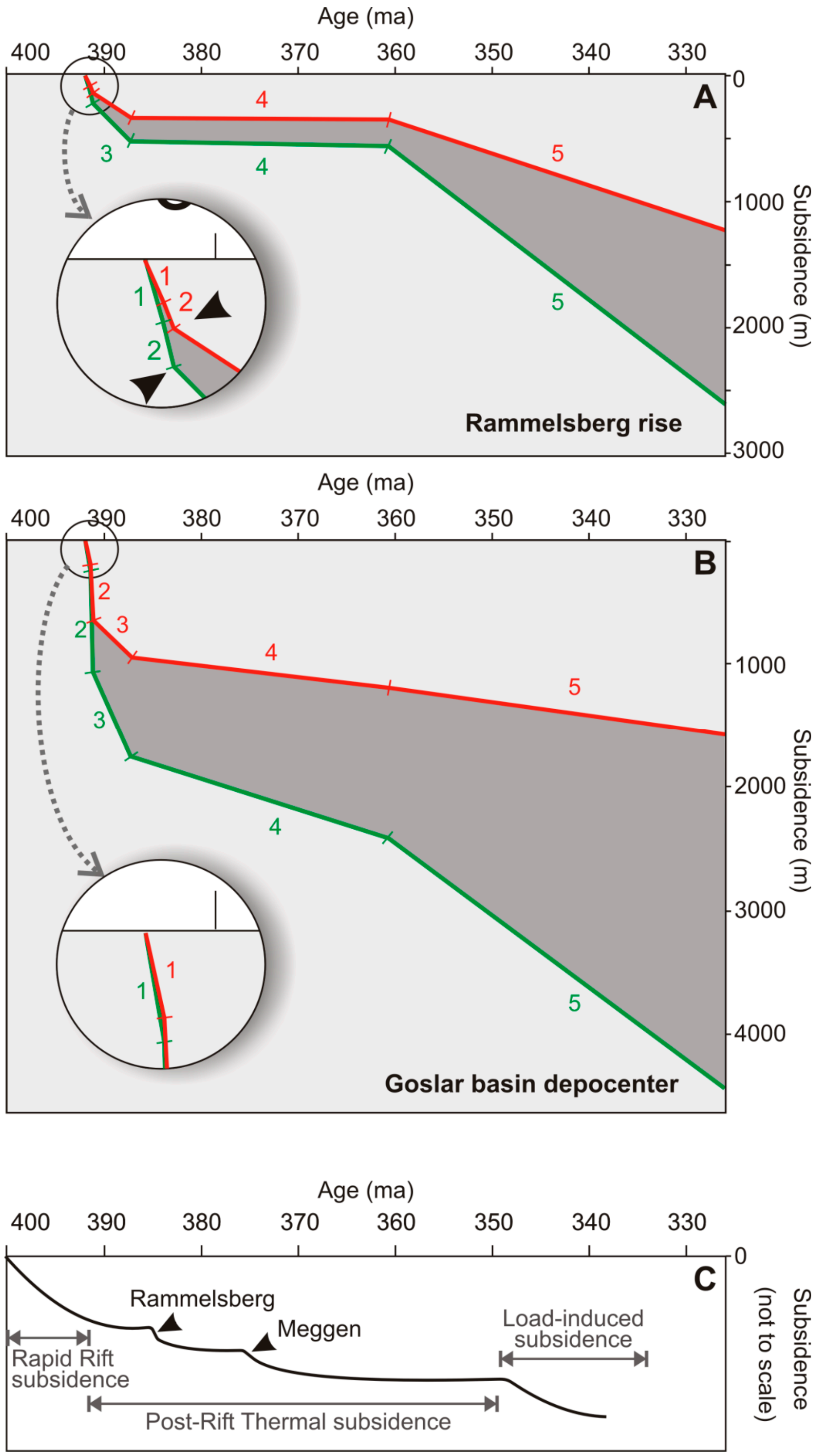


**Figure 4.** Total accommodation (green) and tectonic subsidence (red) curves for the Rammelsberg rise (**A**) and Goslar basin depocenter (**B**) indicating the five stages considered in this study; Black arrows show the location of the ore horizon; (**C**) Generalized subsidence curve (with no specification of the subsidence type, location and thickness) for the Rhenish Massif, after Large [3].

In general, the two subsidence curves here analyzed show two initial short and steep segments that become more gently steep and longer at the end of the curve. The Rammelsberg massive sulfides are located just at the inflection point. Subsidence curves for passive margins depict similar trends [8,28] but, in those cases, the time considered is significantly longer.

In detail, stages 1 and 2 for depocenter and margin curves represent two short and highly subsiding episodes comparable to the rapid subsidence events described by Vannucchi et al. [63] or Vilas et al. [25]. Analyzing each pair of segments independently, it is noteworthy that the segments for total accommodation and tectonic subsidence in the first stage are almost similar, indicating that subsidence was mostly of tectonic origin. This was probably related to the Variscan crustal stretching that compares with the initial subsidence stage by McKenzie [23]. By contrast, the segments in stage 2, which are otherwise somewhat steeper than those in stage 1, clearly differ in length. This points to an origin not-exclusively tectonic. Whereas in the depocenter, the sediment load can be alluded as a complementary mechanism to explain the total subsidence, the small amount of sediments deposited in the Rammelsberg ridge does not satisfy this hypothesis. The paleogeographic location of Rammelsberg at the basin margin and just above the Balve–Obersheld fault zone favored an increasing heat flow [22]. Therefore, the additional mechanism proposed for the generation of accommodation space in this area is thermal subsidence.

The geodynamic evolution of depocenter and basin margin clearly diverge from this stage on. As a consequence, the difference between the accommodation rates at both areas reaches here its maximum value (Table 1). The third stage is defined by segments with clearly different lengths and slopes. Covering a considerably larger time-span (4 ma approx.), this stage is characterized by the mutual deceleration of total accommodation and tectonic subsidence. At the basin depocenter, the sedimentary loading became the major accommodation mechanism. In the basin margin, the subsidence was caused by tectonic and thermal processes. In this case, a substantial participation of the sediment load is still difficult to justify because the sedimentary pile remained relatively thin.

The position of the Rammelsberg massive sulfides, just at the boundary between stages 2 and 3, entirely agrees with the subsidence mechanisms indicated above. The second subsidence event in stage 2, faster than that of stage 1 and generated by the sum of tectonic and thermal subsidence, probably acted as trigger mechanism for the circulation of fluids trapped in the thick sedimentary pile of the basin [29,39,64,65]. The fluids, already enriched in metals, were then channelized by the Balve–Obersheld fault zone and deposited as sulfides at the sea bottom.

Considering that the environmental conditions at the basin were suitable for sulfide deposition and preservation, the relation between flux of mineralizing fluids and sediment supply determined the way in which the sulfides were either deposited as massive ore or disseminated. Whereas in the Rammelsberg shoulder, close to the Balve–Obersheld fault zone, the sedimentation rate (Table 1) gave rise to deposition and preservation of massive sulfides, in the basin depocenter, the effect of a high distance to source of hydrothermal fluids amplified with a very high sedimentation rate (Table 1) favored the dissemination of sulfides.

The parameters in stage 4 indicate tectonic quiescence but also show strong differences among the accommodation at the depocenter and basin edge. Both areas, minimally subsiding, are respectively characterized by expanded and condensed sequences. The accommodation at the Goslar depocenter was primarily related to the sedimentary load. By contrast, in the Rammelsberg rise, the scarce 33 m of sediments accumulated during circa 27 ma can be compared with the sedimentary hiatuses typically developed during tectonic interludes.

Finally, the stage 5 suggests an increase in the accommodation rate in response to the deposition of the vast Culm flysch sequence of shales and greywackes that, coming from the orogenic front, covered the entire region.

With the independence of the differential chronostratigraphic framework and the unequal extension of stages, the subsidence curve by Large [3], and those presented in this study (Figure 4), essentially differ in the interpretation of the sedimentary record. Large [3] based his subsidence curve on a synthetic regional stratigraphic column and assumed that the Kahleberg Formation formed part of the Goslar basin infill. This explains his anomalously long (circa 10 ma) syn-rift stage. Based on the tectonic and depositional history of this unit, its age, and the correlation with equivalent formations from other Variscan localities as distant as the South Portuguese Zone (SW Iberian Peninsula) and the Moroccan Meseta, we interpret that the infill of the Goslar basin commenced with the Calceola Shales. The Kahleberg Formation represents the basin substrate.

Taking into account the different interpretations mentioned above, stages 1–4 in the two curves here presented, characterized by differential subsidence mechanism, correspond to the post-rift thermal subsidence stage of Large [3]. At the same time, the anomalous tectonic pulse that this author associated with the Rammelsberg deposit could be compared with stages 1 and 2 of the subsidence curve at the basin margin. In this curve, however, the generation of the massive sulfides postdates the highly subsiding event (i.e., the ore deposit is located at the curve inflexion point). Finally, the subsidence stage associated with the Culm deposition is similar in both models.

## 6. Conclusions

The study conducted herein permits the following conclusions to be drawn:

(1) The subsidence analysis of the Goslar basin here presented was performed using data from two different paleogeographic scenarios: the depocenter and the basin margin (Rammelsberg location). A detailed revision of the sedimentological, biostratigraphic, and paleogeographic characteristics of the basin were essential for the accurate construction of the curves in both localities.

(2) The two subsidence curves contain initial short and steep stages that become moderately steep and longer at the end. In detail, both curves are composed of five stages that embrace the entire geodynamic and depositional history of the Goslar basin. Stage 1 represents a rapid tectonic subsidence event linked to the basin break-up. Stage 2 defines a second, more rapid subsidence event that promoted the disparate geodynamic behavior between depocenter and basin margin. At the depocenter, the subsidence was caused by the combined effects of tectonic and sediment load. At the basin margin, the subsidence was tectonic and thermal in origin. Stage 3 is characterized by the deceleration of the tectonic effect in the generation of accommodation space. The main subsidence mechanism in the Goslar depocenter was the sediment load. In the Rammelsberg rise, the subsidence was caused by tectonic and thermal mechanisms, with very scarce participation of the sediment load. Stage 4 represents a quiescent tectonic period. At the basin margin the accommodation was virtually negligible, while at the depocenter the very slow subsidence was mostly caused by sediment load. Finally, during stage 5 the accommodation rate increased in response to deposition of the vast Culm flysch sequence.

(3) The Rammelsberg massive sulfide deposit is located at the boundary between stage 2 and 3, exactly at the inflexion point of the basin margin curve. Its origin is associated with the second and more drastic subsidence event located in stage 2.

(4) This is the first time that a rapid subsidence event is proposed as a trigger mechanism for the activation of the hydrothermal system and for the seismic pumping that transported metal-enriched fluids from reservoir to the seafloor.

(5) Taking apart the environmental conditions of the Goslar basin, the most critical parameter in the generation of the ore deposit was the relation between mineralizing fluid supply and accommodation rate. At the Rammelsberg shoulder, the sedimentation rate favored the generation and preservation of massive sulfides, whereas at the depocenter, the accumulation rate was so high, and the fluid supply so low, that the sulfides were disseminated.

**Author Contributions:** Conceptualization, C.M., F.G. and R.S.; Methodology, C.M.; Software, F.G.; Validation, C.M., F.G. and R.S.; Fieldwork, R.S. and F.G. Writing—Original Draft Preparation, C.M.; English version F.G. Writing—Review and Editing, C.M., F.G., R.S.; Project Administration, C.M., R.S.; Funding Acquisition, C.M., R.S.

**Funding:** This research was funded by the CICYT (Spain) Research Projects CGL2011-30011 and CGL2016-79204-R and the Research Group THARSIS RNM 198-PAI (Junta de Andalucía).

**Acknowledgments:** We are grateful to the chief editor of Minerals and the three anonymous reviewers whose comments significantly improved this paper.

**Conflicts of Interest:** The authors declare no conflicts of interest.

## References

1. Ruffell, A.H.; Moles, N.R.; Parnell, J. Characterisation and prediction of sediment-hosted ore deposits using sequence stratigraphy. *Ore Geol. Rev.* **1998**, *12*, 207–223. [CrossRef]
2. Maynard, J.B.; Klein, G.D. Tectonic subsidence analysis in the characterization of sedimentary ore deposits: Examples from the Witwatersrand (Au), White Pine (Cu), and Molango (Mn). *Econ. Geol.* **1995**, *90*, 37–50. [CrossRef]
3. Large, D.E. The Palaeotectonic setting of Rammelsberg and Meggen, Germany—A basin analysis study. In *The Genesis of Stratiform Sediment-Hosted Lead and Zinc Deposits: Conference Proceedings*; Turner, R.J.W., Einaudi, M.T., Eds.; Stanford University Publications, Geological Sciences: Stanford, CA, USA, 1986; Volume 20, pp. 109–113.
4. Van Wagoner, J.C.; Posamentier, H.W.; Mitchum, R.M., Jr.; Vail, P.R.; Sarg, J.F.; Loutit, T.S.; Hardenbol, J. An overview of the fundamentals of Sequence Stratigraphy and key definitions. In *Sea-Level Changes: An Integrated Approach*; Wilgus, C.K., Hastings, B.S., Kendall, C.G.S.C., Posamentier, H.W., Ross, C.A., Van Wagoner, J.C., Eds.; Special Publications of SEPM: Tulsa, OK, USA, 1988; Volume 42, pp. 39–46, ISBN 0-918985-74-9.
5. Jervey, M.T. Quantitative geological modeling of siliciclastic rock sequences and their seismic expression. In *Sea-Level Changes—An Integrated Approach*; Wilgus, C.K., Hastings, B.S., Kendall, C.G.S.C., Posamentier, H.W., Ross, C.A., Van Wagoner, J.C., Eds.; Special Publications of SEPM: Tulsa, OK, USA, 1988; Volume 42, pp. 47–69.
6. Einsele, G. *Sedimentary Basins. Evolution, Facies and Sediment Budget*, 2nd ed.; Springer: Berlin/Heidelberg, Germany, 2000; ISBN 978-3-642-08544-4.
7. Naylor, M.; Sinclair, H.D. Pro-versus retro-foreland Basins. *Basin Res.* **2008**, *20*, 285–303. [CrossRef]
8. Xie, X.; Heller, P. Plate tectonics and basin subsidence history. *Geol. Soc. Am. Bull.* **2009**, *121*, 55–64. [CrossRef]
9. Heine, C.; Müller, D.; Steinberger, B.; Torsvik, T.H. Subsidence in intracratonic basins due to dynamic topography. *Phys. Earth Planet. Int.* **2008**, *171*, 252–264. [CrossRef]
10. Perrodon, A.; Masse, P. Subsidence, sedimentation and petroleum systems. *J. Petrol. Geol.* **1984**, *7*, 5–26. [CrossRef]
11. Ramos, A.; Sopeña, A.; Sánchez-Moya, Y.; Muñoz, A. Subsidence analysis, maturity modeling, and hydrocarbon generation of the Alpine sedimentary sequence in the NW of the Iberian Ranges, Central Spain. *Cuad. Geol. Iber.* **1996**, *21*, 23–53.
12. Escalona, A.; Mann, P. Sequence stratigraphic analysis of Eocene clastic foreland basin deposits in central Lake Maracaibo using high-resolution well correlation and 3D seismic data. *AAPG Bull.* **2006**, *90*, 581–624. [CrossRef]
13. Bjorlykke, K. *Petroleum Geoscience. From Sedimentary Environments to Rock Physics*, 2nd ed.; Springer: Berlin/Heidelberg, Germany, 2015; ISBN 978-3-642-34131-1.
14. Wood, A.M.; Paton, D.A.; Collier, R.E.L. The missing complexity in seismically imaged normal faults: What are the implications for geometry and production response. In *Industrial Structural Geology: Principles, Techniques and Integration*; Richards, F.L., Richardson, N.J., Rippington, S.J., Wilson, R.W., Bond, C.E., Eds.; The Geological Society Publishing House: Bath, UK, 2015; Volume 421, pp. 213–230, ISBN 978-1-86239-730-9.
15. Hawkes, A.D.; Scott, D.B.; Lipps, J.; Combellick, R. Evidence for possible precursor events of megathrust earthquakes on the west coast of North America. *Geol. Soc. Am. Bull.* **2005**, *117*, 996–1008. [CrossRef]
16. Brodsky, E.E.; Lajoie, L.J. Anthropogenic seismicity rates and operational parameters at the Salton Sea geothermal field. *Science* **2013**, *341*, 543–546. [CrossRef]
17. Suresh Krishnan, P.V.; Duk-Jim, K.; Jungkyo, J. Subsidence in the Kathmandu Basin, before and after the 2015 Mw 7.8 Gorkha Earthquake, Nepal Revealed from Small Baseline Subset-DInSAR Analysis. *GISci. Remote Sens.* **2018**, *55*, 604–621.

18. Cui, Z.D. *Land Subsidence Induced by the Engineering-Environmental Effect*; Springer Nature Singapore Private Limited: Singapore, 2018; ISBN 978-981-10-8040-1.
19. Leach, D.L.; Sangster, D.F.; Kelley, K.D.; Large, R.R.; Garven, G.; Allen, C.R.; Gutzmer, J.; Walters, S. Sediment-Hosted Lead-Zinc Deposits: A Global Perspective. *Econ. Geol.* **2005**, *100*, 561–609.
20. Clout, J.M.F.; Simonson, B.M. Precambrian Iron Formation and Iron Formation-Hosted Iron Ore Deposits. In *Economic Geology 100th Anniversary Volume*; Hedenquist, J.W., Thompson, J.F.H., Goldfarb, R.J., Richards, J.P., Eds.; Economic Geology: New Haven, CT, USA, 2005; pp. 643–679.
21. Altermann, W.; Nelson, D.R. Sedimentation rates, basin analysis and regional correlations of three Neoarchaean and Palaeoproterozoic sub-basins of the Kaapvaal Craton, Northern Cape Province, South Africa. *Sediment. Geol.* **1998**, *120*, 225–256. [CrossRef]
22. Large, D.E. The evaluation of sedimentary basins for massive sulfide mineralization. In *Base Metal Sulfide Deposits*; Friedrich, G.H., Herzig, P.M., Eds.; Springer: Berlin/Heidelberg, Germany, 1988; pp. 2–11.
23. McKenzie, D. Some remarks on the development of sedimentary basins. *Earth Planet. Sci. Lett.* **1978**, *40*, 25–32. [CrossRef]
24. Paola, C. Quantitative models of sedimentary basin filling. *Sedimentology* **2000**, *47*, 121–178. [CrossRef]
25. Vilas, L.; Martín-Chivelet, J.; Arias, C. Integration of subsidence and sequence stratigraphic analyses in the Cretaceous carbonate platforms of the Prebetic (Jumilla-Yecla Region), Spain. *Palaeogeogr. Palaeoclimatol. Palaeoecol.* **2003**, *200*, 107–129. [CrossRef]
26. Cacace, M.; Bayer, U.; Marotta, A.M.; Lempp, C. Driving mechanisms for basin formationand evolution. In *Dynamics of Complex Sedimentary Basins. The Example of the Central European Basin System*; Littke, R., Bayer, U., Gajewsky, D., Nelskamp, S., Eds.; Springer: Berlin/Heidelberg, Germany, 2008; pp. 35–66, ISBN 978-3-540-85085-4.
27. Berra, F.; Carminati, E. Subsidence history from backstripping analysis of the Permo-Mesozoic succession of the Central Southern Alps (Northern Italy). *Basin Res.* **2010**, *22*, 952–975. [CrossRef]
28. Angevine, C.L.; Heller, P.L.; Paola, C. *Quantitative Sedimentary Basin Modeling*; AAPG Continuing Education Course Note; American Association of Petroleum Geologists: Tulsa, OK, USA, 1990; Volume 32. [CrossRef]
29. Mueller, A.G. The Rammelsberg Shale-Hosted Cu-Zn-Pb Sulfide and Barite Deposits, Germany: Linking Sedex and Kuroko-Type Massive Sulfides; Slide Presentation and Explanatory Notes. Available online: https://www.e-sga.org/fileadmin/sga/Mineral_Deposit_Archive/Rammelsberg/Rammelsberg_SGA_MDA.pdf (accessed on 24 December 2018).
30. Tanner, D.C.; Krawczyk, C.M. Restoration of the Cretaceous uplift of the Harz Mountains, North Germany: Evidence for the geometry of a thick-skinned thrust. *Int. J. Earth Sci.* **2017**, *106*, 2963–2972. [CrossRef]
31. Quinn, D.; Meere, P.A.; Wartho, J.A. A chronology of foreland deformation: Ultra-violet laser $^{40}Ar/^{39}Ar$ dating of syn/late-orogenic intrusions from the Variscides of southwest Ireland. *J. Struct. Geol.* **2005**, *27*, 1413–1425. [CrossRef]
32. Kroner, U.; Mansy, J.L.; Mazur, S.; Aleksandrowski, P.; Hann, H.P.; Huckriede, H.; Lacquement, F.; Lamarche, J.; Ledru, P.; Pharao, T.C.; et al. Variscan tectonics. In *The Geology of Central Europe. Volume 1: Precambrian and Palaeozoic*; McCann, T., Ed.; Geological Society: London, UK, 2008; pp. 559–664, ISBN 9781862392465.
33. Werner, W. Synsedimentary faulting and sediment-hosted submarine-hydrothermal mineralization in the late paleozoic Rhenish Basin (Germany). *Geotechnol. Res.* **1989**, *71*, 309.
34. Sawkins, F.J. Extensional tectonics and mid-Paleozoic massive sulfide occurrences in Europe. *Geol. Rundsch.* **1980**, *69*, 849–860. [CrossRef]
35. Muchez, P.; Heijlen, W.; Banks, D.; Blundell, D. Extensional tectonics and the timing and formation of basin-hosted deposits in Europe. *Ore Geol. Rev.* **2005**, *27*, 241–267. [CrossRef]
36. Franke, W. *The Mid-European Segment of the Variscides: Tectonostratigraphic Units, Terrane Boundaries and Plate Tectonic Evolution*; Geological Society, Special Publications: London, UK, 2000; Volume 179, pp. 35–61.
37. Matte, P. Tectonics and plate tectonics model of the Variscan belt of Europe. *Tectonophysics* **1986**, *126*, 329–374. [CrossRef]
38. Sáez, R.; Moreno, C.; González, F.; Almodóvar, G.R. Black shales and massive sulfide deposits: Causal or casual relationships? Insights from Rammelsberg, Tharsis and Draa Sfar. *Miner. Depos.* **2011**, *46*, 585–614.
39. Large, D.E.; Walcher, E. The Rammelsberg massive sulphide Cu–Zn–Pb–Ba-deposit, Germany: An example of sediment-hosted, massive sulphide mineralisation. *Miner. Depos.* **1999**, *34*, 522–538. [CrossRef]

40. Buchholz, P.; Luppold, F.W. Litho-und Biostratigrafie des älteren Mitteldevons im Oberharz. *Z. Ges. Geowiss.* **2008**, *159*, 263–281.
41. Hannak, W.W. Genesis of the Rammelsberg ore deposit near Goslar/Upper Harz, Federal Republic of Germany. In *Handbook of Stratabound and Stratiform Ore Deposits*; Wolf, K.H., Ed.; Elsevier: Amsterdam, The Nederland, 1981; Volume 9, pp. 551–642, ISBN 10 0444414045.
42. Sperling, H. Das Neue Lager der Blei-Zink-Erzlagerstätte Rammelsberg. *Geol. Jahrb.* **1986**, *85*, 5–177.
43. Abt, W. Ein Beitrag Zur Kenntnis Der Erzlagerstatte Des Rammelsberges Aufgrund von Spezialuntersuchungen Der Tuffe Und Der Tektonik. *Z. Geol. Ges.* **1958**, *110*, 152–204.
44. Sperling, H.; Walcher, E. Die Blei-Zink-Erzlagerstätte Rammelsberg. *Geol. Jahrb.* **1990**, *D91*, 1–153.
45. Sangster, D.F. The role of dense brines in the formation of vent-distal sedimentary-exhalative (SEDEX) lead-zinc deposits: Field and laboratory evidence. *Miner. Depos.* **2002**, *37*, 149–157. [CrossRef]
46. Sangster, D.F. Mississippi Valley-type and sedex lead-zinc deposits: A comparative examination. *Trans. Inst. Min. Metall. B* **1990**, *99*, B21–B42.
47. Anger, G.; Nielsen, H.; Puchelt, H.; Ricke, W. Sulfur isotopes in the Rammelsberg ore deposit. *Econ. Geol.* **1966**, *61*, 511–536. [CrossRef]
48. Eldridge, C.S.; Compston, W.; Williams, I.S.; Both, R.A.; Walshe, J.L.; Ohmoto, H. Sulfur isotope variability in sediment-hosted massive sulfide deposits as determined using the ion microprobe Shrimp: I. An example from the Rammelsberg orebody. *Econ. Geol.* **1988**, *83*, 443–449. [CrossRef]
49. Nielsen, H. Sulfur isotope ratios in stratabound mineralizations in central Europe. *Geol. Jahrb.* **1985**, *D70*, 225–262.
50. Lévêque, J.; Haack, U. Pb isotopes of hydrothermal ores in the Harz. *SGA Monogr. Ser. Miner. Depos.* **1993**, *30*, 197–210.
51. Meier, H. Über die Bedeutung der Os-187 Anomalie des Rammelsberger Erzes für die Bildung der Rammelsberger Lagerstätte. *Erzmetall* **1974**, *27*, 482–485.
52. Steckler, M.S.; Watts, A.B. Subsidence of the Atlantic-type Continental Margin off New York. *Earth Planet. Sci. Lett.* **1978**, *41*, 1–13. [CrossRef]
53. Van Hinte, J.E. Geohistory Analysis—Application of Micropaleontology in exploration geology. *AAPG Bull.* **1978**, *62*, 201–222.
54. Sclater, J.G.; Christie, P. Continental stretching: An explanation of the Post-Mid-Cretaceous Subsidence of the Central North Sea Basin. *J. Geophys. Res. Atmos.* **1980**, *85*, 3711–3739. [CrossRef]
55. Bond, G.C.; Kominz, M.A. Construction of tectonic subsidence curves for the early Paleozoic miogeosyncline, southern Canadian Rocky Mountains: Implications for subsidence mechanisms, age of breakup and crustal thinning. *Geol. Soc. Am. Bull.* **1984**, *95*, 155–173. [CrossRef]
56. Allen, P.A.; Allen, J.R. *Basin Analysis: Principles and Application to Petroleum Play Assessment*; Wiley-Blackwell: Hoboken, NJ, USA, 2009; ISBN 978-1-444-30920-1.
57. Hölzel, M.; Wagreich, M.; Faber, R.; Strauss, P. Regional subsidence analysis in the Vienna Basin (Austria). *Aust. J. Earth Sci.* **2008**, *101*, 88–98.
58. Weddige, K. (Ed.) Devon-Korrelationstabelle. In *Senckenbergiana Lethaea*; Springer-Verlag: Berlin, Germany, 1996; Volume 76, pp. 267–286.
59. Weddige, K. Nomenclatorical note. *Rev. Esp. Micropalentol.* **2003**, *35*, 383.
60. Kaufmann, B. Calibrating the Devonian Time Scale: A synthesis of U–Pb ID–TIMS ages and conodont stratigraphy. *Earth Sci. Rev.* **2006**, *76*, 175–190. [CrossRef]
61. Menning, M.; Alekseev, A.S.; Chuvashov, B.I.; Davydov, V.I.; Devuyst, F.-X.; Forke, H.C.; Grunt, T.A.; Hance, L.; Heckel, P.H.; Izokh, N.G.; et al. Global time scale and regional stratigraphic reference scales of Central and West Europe, East Europe, Tethys, South China, and North America as used in the Devonian–Carboniferous–Permian Correlation Chart 2003 (DCP 2003). *Palaeogeogr. Palaeoclimatol. Palaeoecol.* **2006**, *240*, 318–372. [CrossRef]
62. Dallmeyer, R.D.; Franke, W.; Weber, K. (Eds.) *Pre-Permian Geology of Central and Eastern Europe*; Springer: Berlin/Heidelberg, Germany, 1995; ISBN 978-3-642-77518-5.
63. Vannucchi, P.; Sak, P.B.; Morgan, J.P.; Ohkushi, K.; Ujiie, K. The IODP Expedition 334 Shipboard Scientists; Rapid pulses of uplift, subsidence, and subduction erosion offshore Central America: Implications for building the rock record of convergent margins. *Geology* **2013**, *41*, 995–998. [CrossRef]

64. Muchez, P.; Heijlen, W. Origin and migration of fluids during the evolution of sedimentary basins and the origin of Zn-Pb deposits in Western and Central Europe. *J. Geochem. Explor.* **2003**, *78–79*, 553–557. [CrossRef]
65. Werner, W. Examples of structural control of hydrothermal mineralization: Fault zones in epicontinental sedimentary basins—A review. *Geol. Rundsch.* **1990**, *79*, 279–290. [CrossRef]